Toxicology in Vitro 38 (2017) 150–158

Contents lists available at ScienceDirect

Toxicology in Vitro

journal homepage: www.elsevier.com/locate/toxinvit

A new fluorescence-based method for characterizing *in vitro* aerosol exposure systems

Sandro Steiner, PhD *, Shoaib Majeed, MSc, Gilles Kratzer, MSc, Julia Hoeng, PhD, Stefan Frentzel, PhD

Philip Morris International R&D, Philip Morris Products S.A. (part of Philip Morris International group of companies), Quai Jeanrenaud 5, CH-2000, Neuchatel, Switzerland

ARTICLE INFO

Article history:
Received 25 July 2016
Received in revised form 9 September 2016
Accepted 20 September 2016
Available online 21 September 2016

Keywords:
In vitro aerosol exposure
Aerosol exposure system characterization
Aerosol dosimetry
Vitrocell

ABSTRACT

Knowledge of how an *in vitro* aerosol exposure system delivers a test aerosols to the biological test system is among the most crucial prerequisites for the interpretation of exposure experiments and relies on detailed exposure system characterization. Although various methods for this purpose exist, many of them are time consuming, require extensive instrumentation, or offer only limited ability to assess the performance of the system under experimental settings. We present the development and evaluation of a new, highly robust and sensitive fluorometry-based method for assessing the particle size specific delivery of liquid aerosols.

Glycerol aerosols of different mean particle sizes and narrow size distributions, carrying the fluorophore disodium fluorescein, were generated in a condensation monodisperse aerosol generator. Their detailed characterization confirmed their stability and the robustness and reproducibility of their generation. Test exposures under relevant experimental settings in the Vitrocell® 24/48 aerosol exposure system further confirmed their feasibility for simulating exposures and the high sensitivity of the method.

Potential applications of the presented method range from the experimental confirmation of computationally simulated particle dynamics, over the characterization of *in vitro* aerosol exposure systems, to the detailed description of aerosol delivery in test systems of high complexity.

1. Introduction

With the wide commercialization of electronic cigarettes (e-cigarettes), there is a growing interest in evaluating the toxicity of the aerosols they generate (Farsalinos & Polosa, 2014; Riker et al., 2012; Pepper & Eissenberg, 2014; Pisinger & Døssing, 2014), which, in light of attempts to reduce animal experimentation, is projected to involve more and more *in vitro* toxicological studies. However, *in vitro* toxicological assessment of aerosols is technically challenging. It is generally accepted that exposing submersed cell cultures to extracts of aerosols trapped on filters or in solvents cannot, or can only to a very limited extent, simulate the interaction between a native aerosol and the epithelial lining of the respiratory tract, as the collection and processing of a test aerosol inevitably results in changes to its physicochemical properties. In addition, it is well established that the submersed state of cell cultures is not representative of conditions in the respiratory tract (Paur et al., 2008; Panas et al., 2014; Hirsch et al., 2013; Paur et al., 2011; BéruBé et al., 2010).

In consequence, aerosol exposure at the air-liquid interface (ALI) is the preferable approach. This method requires the test aerosols to be conditioned to meet specific requirements of the cell cultures in terms of temperature and humidity, and to be diluted to achieve realistic doses and dose responses (Paur et al., 2008; Grass et al., 2010). This is commonly achieved in aerosol exposure systems, several of which have been developed in the past years (Paur et al., 2008; Thorne & Adamson, 2013). However, whereas their working principles may vary greatly, they share the common property that besides adjusting the relative humidity, temperature and concentration, they potentially also change other aerosol characteristics. This includes, for instance, the particle number-size distribution (Alonso et al., 1999), the total particle mass (Chang et al., 1985) and the partitioning of semi-volatile compounds between particulate matter (PM) and the gas-vapor phase (GVP) (Chang et al., 1985). As the delivery efficiencies of GVP, PM and particles of different sizes must be assumed to not be equal (Fujitani et al., 2015; Ishikawa et al., 2016; Guha, 2008; Sahu et al., 2013), this inevitably influences the aerosol delivery to the biological test system. Predictions of dosing from the physicochemical properties of the original aerosol are therefore highly error-prone, and affect the relevance of *in vitro* studies that require the achieved aerosol delivery to be known, and moreover, to be representative for the targeted region of

Abbreviations: CMAG, condensation monodisperse aerosol generator; DSF, disodium fluorescein; VC24/48, Vitrocell® 24/48 aerosol exposure system; PBS, phosphate buffered saline; PM, particulate matter; GVP, gas-vapor phase; APS, aerodynamic particle sizer; e-cigarettes, electronic cigarettes; GSD, geometric standard deviation; CFP, cambridge filter pad; CV, coefficient of variation; ULOQ, upper limit of quantification; LLOQ, lower limit of quantification.

* Corresponding author.
E-mail address: Sandro.Steiner@pmi.com (S. Steiner).

http://dx.doi.org/10.1016/j.tiv.2016.09.018

the respiratory tract (Ishikawa et al., 2016; Heyder, 2004). Furthermore, a fully reproducible performance of the exposure systems cannot be assumed by implication and in the case of systems that allow exposing multiple cell cultures simultaneously—be it as replicates or for testing serially diluted aerosols (or both)—inaccurate dosing and/or non-uniform aerosol delivery may occur (Adamson et al., 2014).

Literature is available on how various aerosols, including smoke generated by conventional cigarettes, are delivered in *in vitro* exposure systems (Fujitani et al., 2015; Ishikawa et al., 2016; Adamson et al., 2014; Majeed et al., 2014; Kaur et al., 2010; Adamson et al., 2012; Asimakopoulou et al., 2011; Aufderheide et al., 2013; Kim et al., 2013; Scian et al., 2009; Tippe et al., 2002; Wiegand et al., 2015; Fröhlich et al., 2013; Mertes et al., 2013), but only a limited number of these studies focused on water-soluble, liquid aerosols containing low amounts of volatile and semi-volatile compounds, such as those generated by various e-cigarettes (Hajek et al., 2014). In many aspects, such aerosols behave differently than dry powders or combustion products (Koehler et al., 2012; Feng et al., 2015; Marple et al., 1991; Lízal et al., 2010; Mullins et al., 2003), and will as a result be delivered differently in *in vitro* exposure systems. In particular, if a direct toxicological comparison between whole smoke generated by conventional cigarettes and aerosols generated by e-cigarettes is attempted, great care must be taken when establishing comparable doses. Identical or nearly identical protocols for the generation and application of conventional cigarette smoke and e-cigarette aerosol as applied in many studies (Cervellati et al., 2014; Neilson et al., 2015; Scheffler et al., 2015; Shen et al., 2016) cannot be assumed to result in comparable delivery, unless this was confirmed by quantification of aerosol delivery to the exposure chambers or by detailed exposure system characterization.

Exposure system characterization can be approached in two distinct but not exclusive ways: By comparing the aerosol entering the system (or a part of the system) with the aerosol leaving the system (or a part thereof), or by direct quantification of aerosol deposition on relevant internal surfaces of the system. The former approach allows measuring aerosol evolution and deposition on-line, even simultaneously with the exposure of the biological test systems. It suffers, however, from low spatial resolution, as the exact location within the system at which the observed changes arise cannot be determined. Direct quantification of aerosol deposition, although it can be performed on-line (Thorne & Adamson, 2013; Adamson et al., 2012; Wiegand et al., 2015), is usually performed after exposure or in separate experiments specifically dedicated to system characterization. Commonly applied methodologies include for example counting deposited particles using electron microscopy (Panas et al., 2014; Fujitani et al., 2015; Kim et al., 2013; Tippe et al., 2002; Fröhlich et al., 2013), absorbance/colorimetric measurements (Majeed et al., 2014; Scian et al., 2009), or chromatographic procedures (Thorne & Adamson, 2013; Ishikawa et al., 2016; Majeed et al., 2014; Mertes et al., 2013). These methods allow the description of aerosol delivery in an exposure system with an impressive level of detail, and are clearly indispensable for describing the exact dosing of complex multicomponent aerosols. The advantages notwithstanding, these methods are usually time-consuming, expensive, and require extensive analytical equipment and may therefore not be suitable for many institutions performing *in vitro* aerosol exposures. In addition, in many aspects it is advantageous to perform exposure system characterization with model aerosols of low complexity, especially when a mechanistic understanding of the system and not only the aerosol delivery to the exposure chambers is of interest.

In this paper, we describe a method for the quantification of aerosol deposition that, because of its simple but robust character, allows characterizing the aerosol delivery in an aerosol exposure system in detail even if extensive analytical equipment is unavailable. We focused specifically on aerosols comparable to those generated by common types of e-cigarettes, because for this kind of aerosols, only a limited number of established methods for exposure system characterization are available. Since the aerosols generated by e-cigarettes (but also by various medical devices for drug inhalation) contain large amounts of glycerol (Hajek et al., 2014; Watts et al., 2008; Patton & Byron, 2007; Haghi et al., 2014), we chose glycerol as the aerosol material. Fluorometry was used for aerosol detection because of its robustness and simplicity in implementation, disodium fluorescein (DSF) was chosen as the fluorescent label.

As a proof of concept, we applied the method to the Vitrocell® 24/48 aerosol exposure system (VC24/48, VITROCELL Systems GmbH, Waldkirch, Germany), the system we use at our facility for exposing organotypic cell cultures as a part of the toxicological assessment of conventional and novel tobacco products. We thereby focused on the sensitivity of the method and on the dosing accuracy.

2. Materials and methods

2.1. Aerosol generation

Fluorescent aerosols were generated in a TSI 3475 condensation monodisperse aerosol generator (CMAG) (TSI, Shoreview, MN, USA). Its working principle relies on aerosolizing an aqueous salt solution in an atomizer and drying the obtained aerosol in a diffusion dryer, resulting in salt crystals of roughly 100-nm diameter. In a saturator, these salt nuclei are bubbled through heated aerosol material and the obtained nuclei-vapor mixture is subsequently heated in a re-heater unit, where complete evaporation of the aerosol material is assured. Cooling down in a condensation chimney causes super-saturation and homogeneous condensation of the vapor onto the salt nuclei. By varying the temperature in the saturator and the volume flow through the saturator, and by removing a part of the salt nuclei via filtration, the amount of aerosol material per salt nucleus, and thereby the resulting particle size, can be modulated.

For our application, we used a 0.5% aqueous solution of DSF, (Sigma-Aldrich, Munich, Germany) as the source of the salt nuclei, onto which glycerol (>99.5%, Sigma Aldrich) as aerosol material was condensed. The applied CMAG settings are listed in Table 1.

2.2. Aerosol characterization

Various aerosols of different particle number-size distributions could be generated in the CMAG, four of which were selected for more detailed characterization (Table 1).

In eight independent repetitions, particle number-size distributions and their modes, mean aerodynamic particle sizes and their geometric standard deviations (GSDs), and median aerodynamic particle sizes were measured continuously during 20–25 min, using a TSI 3321 Aerodynamic Particle Sizer (APS) with an accessory dilution unit (TSI 3302 A Aerosol Diluter, 100:1 capillary inserted). The APS was set to report data averaged over 10 s, and the obtained 120–150 data points per repetition were averaged for assessing intra- and inter-repetition stability of the aerosol generation.

Particle concentrations were also measured, but as the APS was operated at the upper limits of reliably measureable particle densities, the reported values are expected to underestimate the actual concentrations. Since in addition, the aerosol density was primarily captured by the DSF and aerosol mass flow rates, particle concentrations reported by the APS are not further used as quantitative data.

To derive aerosol mass deliveries in an aerosol exposure system based on fluorometric quantification of DSF delivery, the DSF and aerosol mass flow rates through the system during test exposures need to be determined. This was achieved by trapping the aerosols on weighted Cambridge filter pads (CFPs) (Borgwaldt KC, Hamburg, Germany) for defined periods of time (1–5 min, depending on the aerosol size) followed by determination of the deposited aerosol mass and elution and fluorometric quantification of the deposited DSF. To characterize the four selected aerosols, this was done with the APS, but not the VC24/48 being installed downstream of the CFP-holder. Trapping was

Table 1
Aerosol generation and characterization ($N = 8$).

Nominal mean aerodynamic particle diameter	0.8 μm	1.1 μm	1.4 μm	1.6 μm
CMAG settings				
Total flow (rotameter scale value[a])	8	8	8	8
Saturator flow (rotameter scale value[a])	1.5–2	3.75–4.25	6.75–7.25	7.75–8
Screen flow (rotameter scale value[a])	1	1	1	3.5–4.5
Saturator temperature (°C)	160	160	160	160
Reheated temperature (°C)	340	340	340	340
Aerosol characterization	Average ± SD (CV)	Average ± SD (CV)	Average ± SD (CV)	Average ± SD (CV)
Aerosol mass flow rate (mg/min)	18.9 ± 1.8 (9.6)	42.8 ± 2.1 (5.0)	84.1 ± 3.9 (4.6)	93.0 ± 2.9 (3.2)
DSF mass flow rate (mg/min)	0.102 ± 0.009 (9.1)	0.106 ± 0.021 (20.2)	0.096 ± 0.014 (14.6)	0.065 ± 0.003 (5.1)
Mass ratio DSF/Aerosol	0.0054 ± 0.0007 (12.5)	0.0025 ± 0.0005 (20.3)	0.0011 ± 0.0002 (16.4)	0.0007 ± 0.0000 (5.3)
Mean aerodynamic particle diameter (μm)	0.83 ± 0.02 (3.0)	1.13 ± 0.03 (3.1)	1.41 ± 0.02 (3.1)	1.62 ± 0.03 (1.6)
Median (μm)	0.75 ± 0.02	0.97 ± 0.03	1.24 ± 0.03	1.55 ± 0.04
Mode (μm)	0.72 ± 0.03	0.93 ± 0.03	1.24 ± 0.04	1.66 ± 0.03
GSD	1.29 ± 0.02 (1.6)	1.36 ± 0.02 (1.3)	1.39 ± 0.02 (1.6)	1.36 ± 0.02 (1.7)

[a] Exact volume flow rates for the indicated scale values are specified by TSI. A value of 1 refers to the according valve being completely closed, a value of 8 corresponds to roughly 3.6 L/min.

performed during the APS measurements (*i.e.* APS measurements were interrupted), the APS data therefore describe the same aerosol flows as the CFP data. The aerosols trapped on CFPs were eluted from the filters by incubation in 10 mL Dulbecco's phosphate-buffered saline (PBS) (Sigma-Aldrich) at room temperature in the dark on a horizontal shaker for 30 min. To increase the fluorescent activity of DSF, the pH of the PBS was adjusted to 9 (Kesavan, 2000).

2.3. DSF retrieval from CFPs and interaction with glycerol

The reliable calculation of the aerosol mass delivery in an aerosol exposure system depends on exact values for the DSF- and aerosol mass flow rate and the DSF/aerosol mass ratio, which in turn depends on quantitative elution of DSF from CFPs, *i.e.*, on the absence of significant adsorption of DSF to the CFPs or any interaction between the CFPs and the DSF fluorescence. Since the DSF/aerosol mass ratios are different for different aerosols, the absence of effects of glycerol on the fluorescence of DSF in PBS also had to be confirmed.

DSF recovery from CFPs was assessed by pipetting a 1:1 PBS (pH 9):glycerol solution containing 0.0002 g to 0.125 g of DSF onto CFPs, followed by incubation in the dark until the added solution was fully soaked into the filter. DSF was then eluted in 10 mL PBS (pH 9) for 30 min in the dark on a horizontal shaker and quantified and the retrieved DSF mass was compared with the applied DSF mass. Potential effects of the presence of glycerol on the fluorescence of DSF in PBS were assessed by measuring the DSF fluorescence in DSF dilution series (8×10^{-7} — 0.0002 g/L) in PBS (pH 9) containing 0.02, 0.2, 2, 20, and 200 g/L glycerol.

2.4. Test exposures in the VC24/48

Test exposures in the VC24/48 were conducted i) to confirm aerosol stability under applied conditions, *i.e.*, the absence of relevant changes in the aerosol size-distribution due to, for instance, hygroscopic growth, particle size selective aerosol loss, or particle coalescence; ii) to test for interactions between cell culture inserts and DSF, such as adsorption, which would reduce the DSF recovery when collecting the PBS samples; iii) to test for the possibility for accurate aerosol dosing, and iv) to determine the detection limits of the assay under experimentally relevant conditions.

2.5. Experimental settings; CMAG and VC24/48

The interested reader can find a detailed description of the VC24/48 on the manufacturer's website (www.vitrocell.com). Briefly, the test aerosol passes through the VC24/48 via the dilution system, which is located on top of the exposure module. The exposure module provides 48 exposure chambers, which are grouped into 8 rows of 6 replica positions. Upstream of each row, the aerosol in the dilution system can be diluted with fresh air, resulting in a total of seven aerosol dilutions (one per row) and a negative control exposed to fresh air only that can be tested simultaneously. The aerosol passing the dilution system is sampled by negative pressure into exposure trumpets, which project downwards into the exposure chambers and generate a stagnation flow condition over the biological test system. Throughout all exposures described here, the system was operated under identical settings as during previous experiments for VC24/48 characterization (Majeed et al., 2014), *i.e.* the whole system was kept at 37 °C, the dilution-air was brought to 60 ± 5% relative humidity and the volume flow rate through the exposure trumpets was set to 2 mL for all positions. The dilution-air volume flow rates applied to different experiments are specified in the section below.

2.6. Physical setup CMAG-VC24/48

To simulate exposures of organotypic cell cultures as routinely performed at our facility, the aerosol volume flow rate into the VC24/48 was adjusted to 0.41 L/min, corresponding to a 55 mL puff from a tested tobacco product (according to the Health Canada smoking regimen (Health-Canada, 1999)) provided within 8 s.

A CFP housing in which aerosols could be trapped on their way to the exposure system was installed in the tubings upstream of the VC24/48 (35 cm away from the entry point into the system). This permitted the determination of the aerosol and DSF mass flow rates, as described in the section on aerosol characterization.

As the inflow of diluted air generates a positive pressure within the VC24/48, a vacuum pump downstream of the system was required to establish a constant unidirectional flow. A bifurcation with a needle valve at its open end was installed upstream of the pump. By placing a mass flow meter (0–5 L/min mass flow meter, Aalborg, Orangeburg, NY, USA) upstream the VC24/48, increasing or decreasing the flow of surrounding air through this needle valve allowed setting the volume flow rate entering the VC24/48 (with or without CFP upstream of the system) to exactly 0.41 L/min. Once a stable inflow was reached, the mass flow meter was removed and aerosol trapping or aerosol exposures commenced.

2.7. Aerosol stability

Aerosol stability in the VC 24/48 was confirmed by feeding two of the selected aerosols (0.8 and 1.1 μm mean diameter) through the complete dilution system of the VC24/48. In two independent repetitions, the particle number-size distributions were measured for 2–3 min, alternately upstream and downstream of the system. A serial dilution

was applied in the VC24/48, the cumulative dilution-air volume flow rates from rows 1–7 being set to 0.1, 0.2, 0.5, 1, 1.5, 2, and 3 L/min, resulting in aerosol concentrations of 81, 67, 45, 29, 22, 17, and 12% compared with the CMAG output. When measuring aerosol parameters downstream of the VC24/48, the APS served as a pump that generated the constant unidirectional flow through the system. Flow regulation was achieved analogously to what is described above.

2.8. DSF recovery from cell culture inserts

DSF recovery from cell culture inserts was assessed by placing ThinCert™ cell culture inserts (24-well format, transparent insert membrane, 0.4 μm pore diameter; Greiner Bio-One, Kremsmünster, Austria) containing 100 μL PBS (pH 9) and 10–250 mg/L DSF in one row of the exposure module; the inserts were exposed to filtered air, without feeding aerosol into the system, for 28 min (the duration we apply in regular exposures of organotypic cell cultures to aerosols generated by tobacco products). PBS samples were then collected, the retrieved DSF concentration was measured and compared with the applied concentration. The flow through the exposure chambers is independent of the flow regimen in the dilution system, therefore no specific dilution scheme was applied; the dilution-air flow was set to 0.5 L/min in row one without any further input in subsequent rows.

2.9. Aerosol dosing and sensitivity limits

To assess the dose response in aerosol delivery to cell culture inserts and for identifying potential sensitivity limits, ThinCert™ cell culture inserts, each containing 100 μL PBS (pH 9), were placed into the exposure module at specified positions. PBS samples served as surrogates for cell cultures, providing an aqueous surface comparable to the mucus layer present on organotypic cultures of airway epithelial cells.

To confirm the linear increase in the aerosol delivery with increasing exposure duration, PBS samples present at positions 1–6 of rows 3 and 5 were exposed to aerosols for 3, 6, 9, 12, 15, 18, and 21 min. Only the aerosol of 0.8 μm mean aerodynamic particle diameter was used, and a dilution-air volume flow rate of 1.5 L/min (resulting in an aerosol concentration of 22%) was applied at the inlet to the first row of the VC24/48 dilution system. To confirm the reproducible aerosol generation, and to calculate the aerosol mass delivery, aerosol was trapped on CFPs and aerosol and DSF mass flow rates and aerosol size measurements were determined before the 3,15, 18 and 21 min exposure.

As during exposures of organotypic cell cultures in the VC24/48 the dosing is usually not achieved by varying the exposure duration, but by serially decreasing the applied aerosol concentration, dilution effects were of greater interest than time-dependent dosing. Accordingly, time-dependent dosing was only measured in one repetition and more focus was put on dilution-dependent dosing. For dilution-dependent dosing, 0.8 μm and 1.6 μm aerosols were used, with the cumulative dilution-air volume flow rates in rows 1–7 set to 0.1, 0.2, 0.5, 1, 1.5, 2, and 3 L/min (81, 67, 45, 29, 22, 17, and 12% aerosols compared with the CMAG output). Cell culture inserts containing PBS samples were placed at positions 1–6 of rows 1–7 and exposed over 28 min. Aerosol trapping on CFPs for the determination of aerosol and DSF mass flow rates and confirmatory particle size measurement was performed before, during, and after the exposures; *i.e.*, the exposures were interrupted after 14 min, mean aerodynamic particle size and GSD were measured, aerosol samples were trapped on CFPs, and exposures were then continued for another 14 min. In total, four experimental repetitions were performed.

In each case, loaded CFPs were washed in 10 mL PBS (pH 9) at room temperature for 30 min in the dark on a horizontal shaker. PBS samples retrieved from individual cell culture inserts were collected and stored at 4 °C in the dark until further processing.

2.10. Fluorescence measurements

Irrespective of the origin of the sample, fluorescence measurements were performed in the same manner: 80 μL sample volumes were pipetted into individual wells of black 96-well microplates with a clear bottom (ViewPlate-96, PerkinElmer, Waltham, MA, USA). Standard curves for converting the fluorescence readout to DSF concentrations (the highly robust linear range covered 0.2 to 10^{-4} mg/L, as determined empirically) were generated on each plate using PBS (pH 9). Required sample dilutions were determined empirically.

Fluorometric measurements were performed in a FLUOstar Omega Microplate Reader (BMG Labtech, Ortenberg, Germany) at an excitation wavelength of 485 nm and an emission wavelength of 520 nm (top optics reading, gain adjustment in the well containing the highest standard, fast reading mode). Blank correction for samples retrieved from the VC24/48 was based on the fluorescence of pure PBS (pH 9). For the background correction when measuring DSF eluted from CFPs, PBS (pH 9) in which an unloaded CFP was incubated for 30 min on a horizontal shaker served as a blank.

2.11. Data processing

Primary readout for all samples was the DSF concentrations in the collected PBS samples, which were converted to DSF masses based on the known sample volumes. Using the time period during which aerosol was trapped on CFPs, DSF mass flow rates were calculated according to Eq. 1.

$$DSF\ mass\ flow\ rate = \frac{measured\ DSF\ concentration \times eluate\ volume}{trapping\ time.} \quad (1)$$

Using the aerosol mass flow rate determined by weighting the trapped aerosol, the DSF content of the aerosols was further calculated (Eq. 2)

$$Mass\ ratio\frac{DSF}{aerosol} = \frac{DSF\ mass\ flow\ rate}{aerosol\ mass\ flow\ rate} \quad (2)$$

Using the DSF masses delivered to a given position within the VC24/48, absolute aerosol mass deliveries were calculated according to Eq. 3.

$$Absolute\ aerosol\ mass\ delivery = \frac{DSF\ mass\ detected\ at\ position\ XY}{Mass\ ratio\frac{DSF}{Aerosol}} \quad (3)$$

2.12. Statistical analysis

2.12.1. Control assessment

Linearity assessments were performed using the least squares method with constrained null y-intercept. The coefficients of determination (R^2) are systematically reported as a goodness-of-fit measurement.

2.12.2. Aerosol generation

Aerosol characterization was assessed using coefficients of variation (CV) considering independent repetitions of aerosol generation.

3. Results

3.1. Aerosol generation and characterization

Empirical testing of various CMAG settings resulted in a number of aerosols that could be generated and kept stable over time. Four aerosols with mean aerodynamic particle sizes of 0.8, 1.1, 1.4, and 1.6 μm were selected for further characterization and for test exposures in the VC24/48. The CMAG settings, as well as relevant measured aerosol

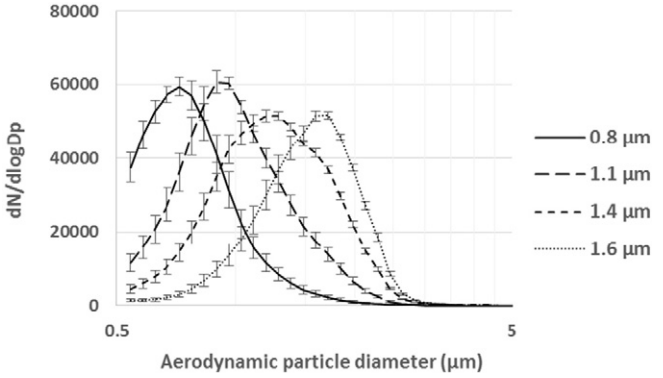

Fig. 1. Particle number-size distributions of the aerosols generated in the condensation monodisperse aerosol generator (CMAG). Error bars indicate standard deviations.

parameters, are listed in Table 1, the particle number-size distributions of the selected aerosols are shown in Fig. 1. As shown in Fig. 2 and Table 1, the aerosols' number-size distributions were highly reproducible, both within and between repeated runs of generation. However, monodispersity of the aerosols was not reached, as GSDs were in the range of 1.3–1.4, and considerable overlaps in the number-size distributions of the different aerosols were observed, which decreases the sensitivity with which particle size-specific effects (*e.g.*, the size-specific aerosol delivery in exposure systems) can be detected. At least for large differences in the mean aerodynamic particle size (roughly 500 nm and higher), this was still possible however, as a clear difference in the delivery efficiency of the 0.8 µm and the 1.6 µm aerosols was detectable (data not shown). Overall, aerosol and DSF mass flow rates, and accordingly DSF/aerosol mass ratios, were less reproducible than the aerosol size parameters (Table 1). As expected, the aerosol mass flow rate increased strongly with increasing mean particle size, whereas the DSF mass flow rate was comparable for the 0.8, 1.1, and 1.4 µm aerosol (but lower for the 1.6 µm aerosol, because of the removal of DSF nuclei in the CMAG). Accordingly, the DSF/aerosol mass ratio decreased strongly with increasing mean particle size.

3.2. DSF retrieval from CFPs and interaction with glycerol

Washing CFPs artificially loaded with aerosol material in PBS consistently resulted in a higher fluorescence yield than expected based on the DSF masses applied to the filters. As the only possible source of the surplus fluorescence was the filters themselves, separate blank corrections for the CFPs were introduced: Unloaded CFPs were processed in parallel with the loaded ones and were included in all measurements in later steps. Fig. 3A shows the DSF recovery from CFPs after blank corrections. The mean of the ratio of measured to expected fluorescence yield over all data points was 1.069 ± 0.009, which confirmed quantitative DSF recovery from Cambridge filters over a broad range of DSF concentrations.

At very high glycerol concentrations (200 g/L), an effect on the fluorescence of DSF in PBS could be detected, but this applied only to the lower range of accessible DSF concentrations, *i.e.*, below 1 µg/L (Fig. 3B). For 20 g/L glycerol, the effect was not observed. A deposition of 20 g aerosol but only 1 µg DSF per liter PBS was not reached under relevant conditions, as evidenced by the aerosol mass deliveries measured in the VC24/48 (described below) and the measured DSF/aerosol mass ratios (Table 1), glycerol effects were therefore considered irrelevant.

3.3. Test exposures in the VC24/48

3.3.1. DSF recovery from cell culture inserts

Over the whole range of DSF concentrations assessed (10–250 mg/L), the results show a strong linear correlation between the expected fluorescence (added to cell culture inserts prior to exposure to fresh air in the VC24/48) and the detected fluorescence (measured upon exposure to fresh air), but that a higher fluorescent activity was retrieved than added (Fig. 3C). The linear fit shows a slope of 1.207 ± 0.026, which is interpretable as the corrected average ratio of measured to expected fluorescence retrieval over all data points. Exposure of pure PBS did not result in any detectable fluorescent signal, so the VC24/48 and the cell culture inserts were ruled out as sources for the excess fluorescence. The slight increase in the DSF concentrations of the PBS samples was in fact expected, because when exposed to air of 60% relative humidity over 28 min at 37 °C, evaporation of a small volume of water (but not DSF) from the samples will occur. This effect introduces an over-estimation of aerosol delivery, which, although not done in the present work, could be corrected by determining the volume change in the PBS samples.

3.3.2. Aerosol stability in the VC24/48

APS measurements up- and downstream the V24/48 revealed no relevant changes in the particle size distributions (Fig. 3D), but a higher particle concentration downstream the VC24/48 compared to upstream the system. This was the result of the physical setup used for aerosol sampling up- and downstream the VC24/48 not being identical, and since in addition, the APS was operated at the upper limit of feasible

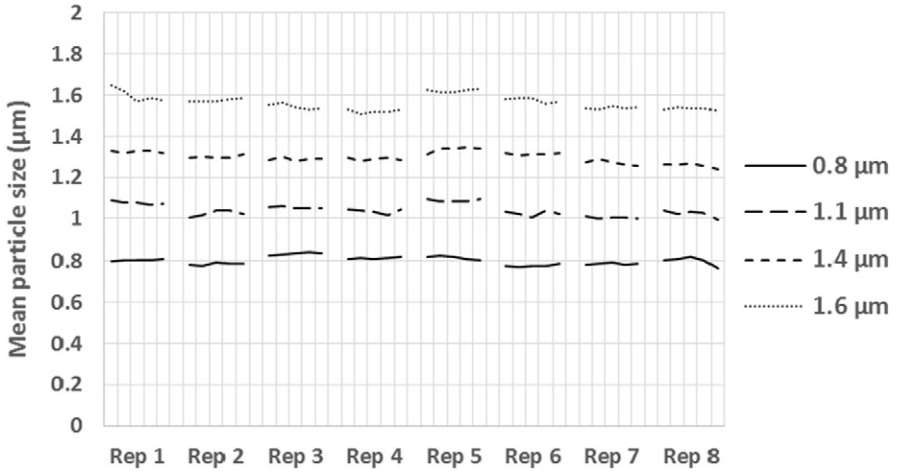

Fig. 2. In eight independent repetitions of aerosol generation, the aerosol mean aerodynamic particle diameters were continuously monitored with an aerodynamic particle sizer (APS). Extracts of the measured data (five values reported by APS, each the average over ten seconds acquisition time) are displayed to demonstrate the aerosol size stability over time and the aerosol size reproducibility across the repetitions.

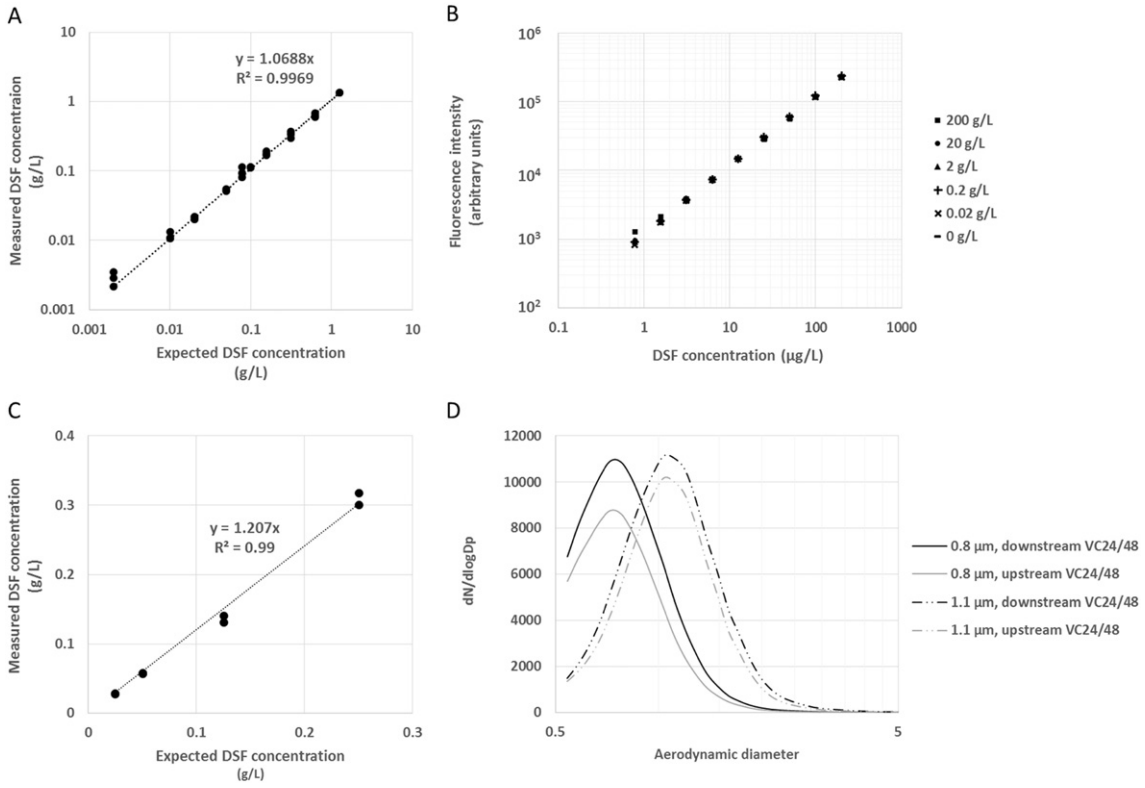

Fig. 3. Control experiments for testing disodium fluorescein (DSF) retrieval and aerosol stability. A) DSF recovery from Cambridge filter pads (CFPs). Three independent measurements (2 for 1.25 and 0.05 g/L) were performed. The dotted line represents the linear fit to the data. Its slope and R^2 are indicated in the plot and demonstrate quantitative DSF retrieval. B) Effect of glycerol on DSF fluorescence. The fluorescence of DSF at various concentrations was tested in presence of 0 to 200 g/L glycerol. An effect was only detected at the lowest DSF concentration in the presence of the highest glycerol concentration. C) DSF retrieval from cell culture inserts after exposure to filtered humidified air in the Vitrocell® 24/48 aerosol exposure system (VC24/48). Per tested DSF concentration, three samples were exposed simultaneously in a single repetition. The dotted line represents the linear fit to the data; its slope and R^2 are indicated in the plot. The retrieved fluorescence was slightly higher than expected, which is assumed to be a result of evaporation of water from the phosphate-buffered saline samples in the inserts. D) Particle number-size distributions of two of the used aerosols, measured up- and downstream of the VC24/48 using an aerodynamic particle sizer (APS). No change in the aerosol size was detected.

aerosol concentrations (which may result in under-estimated values for the particle concentrations, but does not affect the reported size distribution) represents an artifact of the applied experimental settings.

3.3.3. Aerosol dosing in the VC24/48

Decreasing the exposure duration, as well as decreasing the aerosol concentration, resulted in decreased aerosol mass delivery to the exposed PBS samples (Figs. 4 and 5). Twenty-one minutes of exposure resulted in 8.6 µg, and 3 min of exposure resulted in 1.4 µg aerosol delivery per cell culture insert (both measured in pooled PBS samples retrieved from the 12 inserts exposed in rows 3 and 5). Linear regression gave an R^2 value of 0.95. For the 0.8 µm aerosol and 1.6 µm aerosol, exposure to 82% aerosol over 28 min resulted in 97.0 ± 39.0 µg and 386.0 ± 76.0 µg aerosol delivered per cell culture insert. The corresponding values measured for 12% aerosol are 15.4 ± 3.7 µg and 57.8 ± 10.7 µg (each an average of six positions per row over three repetitions). The R^2 values for a linear relationship between aerosol concentration and delivery were 0.97 (0.8 µm aerosol) and 0.96 (1.6 µm aerosol).

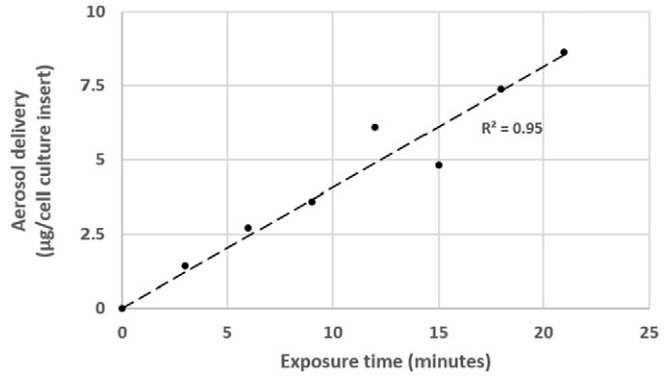

Fig. 4. Aerosol mass delivery to cell culture inserts as a function of exposure time. Time-dependent dosing was only assessed for the aerosol of 0.8 µm mean aerodynamic diameter at a dilution-air volume flow rate of 1.5 L/min (22% aerosol) in a single experimental repetition. The points represent the mean aerosol mass delivered per position of two dilution rows (phosphate buffered saline samples retrieved from 12 replica positions were pooled). The dashed line represents the linear fit to the data.

3.3.4. Assay sensitivity, detection limits

The linear range of the DSF standard curves, defining the lower and upper limit of quantification (LLOQ, ULOQ) covered the DSF concentration range from 200 down to 0.1 µg/L. At 0.1 µg/L, raw fluorescence intensity readouts ranged from 480 to 580, and PBS blanks yielded values ranging from 270 to 360. The noise originating from the microplates and/or the fluorometer (*i.e.* readout from empty wells) was in the range of 50.

As expected, with 1.4 µg per position, the lowest aerosol mass delivery was measured at 3 min of exposure to 22% aerosol (0.8 µm mean aerodynamic diameter). In this particular case, the DSF/aerosol mass ratio was 0.0053, and the DSF concentration in the 100 µL PBS samples was 0.075 µg/L and therefore below the limits of quantification. All other measured DSF concentrations, however, were within the linear range of the standard. For instance, a 6-min exposure to 22% aerosol (0.8 µm) resulted in DSF concentrations of 0.143 µg/L. Exposure to 12% aerosol of the lowest DSF content (1.6 µm mean aerodynamic diameter,

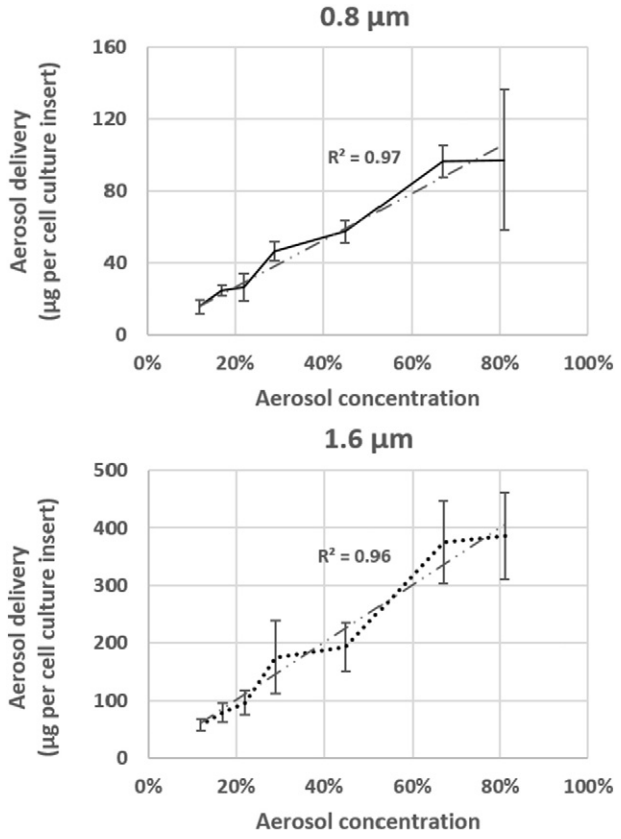

Fig. 5. Aerosol mass delivery as a function of aerosol concentration. Two aerosols, 0.8 µm and 1.6 µm in mean aerodynamic diameter, were used for exposing phosphate-buffered saline samples in cell culture inserts in the Vitrocell® 24/48 aerosol exposure system. Serial aerosol dilution was achieved by applying cumulative dilution-air flow rates of 0.1, 0.2, 0.5, 1, 1.5, 2, and 3 L/min in dilution rows 1–7 (corresponding to 81, 67, 45, 29, 22, 17, and 12% aerosol relative to the condensation monodisperse aerosol generator output). Error bars indicate standard deviations; $N = 4$. The dashed lines represents the linear fit to the data (R^2 values are indicated).

with a DSF/aerosol mass ratio of 0.0009) over 28 min resulted in an aerosol mass delivery of 57.8 ± 10.7 µg per position, and a DSF concentration of 400 µg/L – 4000-fold higher than the LLOQ.

4. Discussion

A variety of methods for characterizing the deposition of aerosols in exposure systems have been developed and applied over the years (Panas et al., 2014; Thorne & Adamson, 2013; Fujitani et al., 2015; Ishikawa et al., 2016; Majeed et al., 2014; Kim et al., 2013; Scian et al., 2009; Tippe et al., 2002; Wiegand et al., 2015; Fröhlich et al., 2013; Mertes et al., 2013; Lízal et al., 2010; Lizal et al., 2012; Bowes & Swift, 1989; Belka et al., 2014), and all of them provide valuable tools for exposure system characterization and *in vitro* dosimetry. The assay introduced here is in many aspects comparable to existing fluorescence-based methods (Lízal et al., 2010; Lizal et al., 2012; Bowes & Swift, 1989; Belka et al., 2014), but the combination of fluorometric aerosol detection with liquid, water-soluble aerosols that can be generated in a particle size-specific manner offers new possibilities: Particle size-specific aerosol deposition covering a wide range of sizes has so far mainly been investigated using solid particles, which in many aspects are not fully representative of liquid aerosols (Koehler et al., 2012; Marple et al., 1991; Lízal et al., 2010; Mullins et al., 2003). In addition, the possibility to generate easily traceable aerosols of tunable particle size distribution allows modeling a variety of aerosols of interest and therefore studying their dynamics in an efficient and unbiased manner. In addition, because of the high water solubility of DSF and glycerol, deposited aerosol can quantitatively be washed off any internal system parts using aqueous solvents. This could be exploited for quantifying aerosol losses within an aerosol exposure system and, in combination with the virtual non-toxicity of glycerol and DSF (Yannuzzi et al., 1986), allows minimizing the risk of introducing system memory effects that might influence biological responses in later exposure experiments.

The key prerequisites for a method for characterizing an aerosol exposure system are: i) the robustness and sensitivity with which the delivered model aerosol can be quantified, ii) the robustness with which the model aerosol can be generated and delivered to the exposure system, and iii) the degree to which the model aerosol is representative of aerosols to be tested in real-life experiments. Provided that these requirements are fully met, simulating and quantifying potential biases resulting from the exposure system is feasible, and identifying optimal system operation conditions under which a minimal system-related bias to the exposures can be achieved is possible.

The high sensitivity of fluorometric DSF quantification was demonstrated in the test exposures in the VC24/48, as the DSF concentrations measured in exposed PBS samples were commonly orders of magnitude higher than required for accurate quantification. Sensitivity issues arise only if exposure durations are kept very short, and mainly if highly diluted aerosols are used. Furthermore, possible sources of bias, such as the potential interference of glycerol with the fluorescence of DSF or the interaction of DSF with either CFPs or cell culture inserts, have been tested and found not to affect the results. Although the method may overestimate the aerosol mass delivery slightly, likely because of water evaporation from the test samples, this effect can be eliminated by correcting for the samples' volume change. Since, in addition, the composition and the pH of PBS is stable, and because DSF is a robust fluorophore of relatively weak light sensitivity (Kesavan & Doherty, 2000; Weidner et al., 2011), the fluorometric quantification of aerosol deposition can be considered unbiased by environmental effects.

The robustness of the aerosol generation with respect to the particle number-size distribution and the mean particle diameters and their GSDs was confirmed, both over time within individual runs and between individual runs of aerosol generation.

Larger variations were observed for the aerosol and DSF mass flow rates, and hence for the DSF content of the aerosols. Differential filtration efficiencies of individual CFPs and fluctuations in the CMAG output cannot be ruled out by implication as causes for these variations. A salt concentration of 0.5% in the atomizer is beyond what is recommended by the manufacturer, and could be a reason for the observed variations, hence decreasing the DSF concentration could potentially increase the reproducibility of the DSF mass flow rate, which will be further pursued. Given that the delivered aerosol masses were orders of magnitude higher than required for quantitative detection, a more than tenfold decrease in the salt concentration in the atomizer would be fully applicable.

Notably, the variations are unlikely to affect reproducibility of test exposures by changing basic aerosol dynamics. Aerosol concentration (that is, the mass flow rate) did not differ by more than 20% between individual repetitions of aerosol generation and variations in the DSF content of the aerosols are not expected to have a detectable effect, as the aerosol dynamics are determined by glycerol, which even for the aerosol of highest DSF content accounted for more than 99% of the particle mass. Furthermore, aerosol and DSF mass flow rates, as well as the DSF/aerosol mass ratios, are required for correcting the measured DSF delivery within the exposure system and for converting fluorescence measurements to delivery efficiencies and absolute mass deliveries. Variations in the DSF and aerosol mass flow rates and the DSF/aerosol mass ratio are therefore corrected automatically. However, it is evident that for reliable calculation of delivery efficiencies and absolute mass deliveries, aerosol characterization has to be performed during each test exposure, preferably at a higher frequency than it was done in this work.

The test exposures in the VC24/48 demonstrated that the generated glycerol aerosols provide a feasible model for simulating exposure

experiments. Independently of the aerosol concentration, their particle number-size distributions were stable along their passage through the system and the application of different aerosol concentrations was reflected in differential aerosol deliveries. Moreover, even though not investigated in detail, we observed different aerosol delivery efficiencies for the 0.8 μm and the 1.6 μm aerosol in the test exposures with serial aerosol dilution, which can only be interpreted as the result of the different particle sizes. Although the cause of the lower delivery efficiency of larger aerosols could not be derived from the current, limited data set, the fact that it could be observed strongly indicates that with the method presented here, mechanistic properties of aerosol exposure systems can be detected with high sensitivity.

Whether the last criterion listed above—the degree to which the model aerosol is representative of the aerosols to be tested in exposure experiments—is fulfilled, cannot be determined solely from the results presented here.

In general, the complete absence of a traceable GVP in the DSF-labeled glycerol aerosols is advantageous if the dynamics of the particulate fraction are of interest; *i.e.*, if a mechanistic understanding of the particle delivery behavior of an exposure system is attempted. It clearly limits, however, the suitability of the method for modeling the total delivery of an aerosol containing relevant amounts of volatile and/or semi-volatile compounds. Our focus was the simulation of liquid aerosols, such as the ones generated by e-cigarettes (Hajek et al., 2014), which are rich in glycerol and very poor in GVP constituents (Schripp et al., 2013; Goniewicz et al., 2014). With regard to the toxicological assessment of e-cigarettes, DSF-labeled glycerol aerosols therefore provide a suitable model system for both, describing particle dynamics within the exposure system as well as the overall aerosol delivery.

Given the advantages and the performance of the method as described above, it potentially also provides an optimal approach for studying the delivery of other types of liquid particles within an exposure system and the system's mechanistic properties, however: The aerosols generated by e-cigarettes are comparable to the aerosols generated by various medical inhalation devices (Watts et al., 2008; Patton & Byron, 2007; Haghi et al., 2014), and fluorometric methods are also applicable in physical models of the human respiratory tract (Lízal et al., 2010; Lizal et al., 2012; Belka et al., 2014), or even of the human oral airways (Bowes & Swift, 1989). Nonetheless, for other aerosol types, feasibility would have to be determined individually. For any application, we recommend that the delivery of the test aerosol is determined experimentally for a few basic settings of the exposure system, and compared with the delivery of the model aerosol used for test exposures. If the comparison meets pre-defined acceptance criteria, the model aerosols can be used to simulate any exposure system setting of interest.

In summary, we have developed an approach for aerosol exposure system characterization that offers a method for investigating particle dynamics within exposure systems in a particle size specific manner. Its applicability, robustness, and sensitivity have been confirmed under realistic exposure conditions, using the Vitrocell® 24/48 aerosol exposure system as a test system.

The model aerosols we used are of low complexity and high stability, and can therefore be characterized in detail. They offer the possibility of investigating mechanistic properties of aerosol exposure systems without interference from dynamic changes in the aerosols. Although specifically designed for characterizing exposure systems for their use in the toxicological assessment of e-cigarettes, the approach is not limited to this application. Results obtained by this method are representative for liquid, glycerol-rich aerosols, comparable to the ones generated by various electronic tobacco products, but also by a large number of medical devices for drug inhalation. The fluorometric detection of aerosol deposition represents a fast, cost-efficient, and reliable analytical method that does not require extensive analytical equipment and is therefore suitable for any research institution. Consequently, this method represents a valuable tool in a broad field of applications, ranging from the experimental confirmation of computationally simulated particle dynamics, over the characterization of *in vitro* aerosol exposure systems, to the detailed description of aerosol delivery in test systems of high complexity.

Competing interests

Authors are employees of Philip Morris International. Philip Morris International is the sole source of funding and sponsor of this project.

Acknowledgments

We thank Edanz Group Ltd. for their editorial assistance during the development of this manuscript.

References

Adamson, J., et al., 2012. Real-time assessment of cigarette smoke particle deposition *in vitro*. Chemistry Central Journal 6 (1), 98.
Adamson, J., et al., 2014. An inter-machine comparison of tobacco smoke particle deposition *in vitro* from six independent smoke exposure systems. Toxicol. in Vitro 28 (7), 1320–1328.
Alonso, M., et al., 1999. Aerosol particle size growth by simultaneous coagulation and condensation with diffusion losses in laminar flow tubes. J. Aerosol Sci. 30 (9), 1191–1199.
Asimakopoulou, A., et al., 2011. Characterization of a multiculture in-vitro cell exposure chamber for assessing the biological impact of diesel engine exhaust. in InternationalConferenceonSafeProductionandUseofNanomaterials. J. Phys.
Aufderheide, M., et al., 2013. The CULTEX RFS: a comprehensive technical approach for the in vitro exposure of airway epithelial cells to the particulate matter at the air-liquid interface. Biomed. Res. Int. 2013.
Belka, M., et al., 2014. Comparison of methods for evaluation of aerosol deposition in the model of human lungs. in EPJ Web of Conferences. EDP Sciences.
BéruBé, K., et al., 2010. Human primary bronchial lung cell constructs: the new respiratory models. Toxicology 278 (3), 311–318.
Bowes III, S.M., Swift, D.L., 1989. Deposition of inhaled particles in the oral airway during oronasal breathing. Aerosol Sci. Technol. 11 (2), 157–167.
Cervellati, F., et al., 2014. Comparative effects between electronic and cigarette smoke in human keratinocytes and epithelial lung cells. Toxicol. in Vitro 28 (5), 999–1005.
Chang, P.-T., Peters, L.K., Ueno, Y., 1985. Particle size distribution of mainstream cigarette smoke undergoing dilution. Aerosol Sci. Technol. 4 (2), 191–207.
Farsalinos, K.E., Polosa, R., 2014. Safety evaluation and risk assessment of electronic cigarettes as tobacco cigarette substitutes: a systematic review. Therapeutic advances in drug safety 5 (2), 67–86.
Feng, Y., Kleinstreuer, C., Rostami, A., 2015. Evaporation and condensation of multicomponent electronic cigarette droplets and conventional cigarette smoke particles in an idealized G3–G6 triple bifurcating unit. J. Aerosol Sci. 80, 58–74.
Fröhlich, E., et al., 2013. Comparison of two in vitro systems to assess cellular effects of nanoparticles-containing aerosols. Toxicol. in Vitro 27 (1), 409–417.
Fujitani, Y., et al., 2015. Particle deposition efficiency at air–liquid interface of a cell exposure chamber. J. Aerosol Sci. 81, 90–99.
Goniewicz, M.L., et al., 2014. Levels of selected carcinogens and toxicants in vapour from electronic cigarettes. Tob. Control. 23 (2), 133–139.
Grass, R.N., et al., 2010. Exposure of aerosols and nanoparticle dispersions to in vitro cell cultures: a review on the dose relevance of size, mass, surface and concentration. J. Aerosol Sci. 41 (12), 1123–1142.
Guha, A., 2008. Transport and Deposition of Particles in Turbulent and Laminar Flow.
Haghi, M., et al., 2014. Towards the bioequivalence of pressurised metered dose inhalers 2. Aerodynamically equivalent particles (with and without glycerol) exhibit different biopharmaceutical profiles in vitro. Eur. J. Pharm. Biopharm. 86 (1), 38–45.
Hajek, P., et al., 2014. Electronic cigarettes: review of use, content, safety, effects on smokers and potential for harm and benefit. Addiction 109 (11), 1801–1810.
Health-Canada, 1999. Determination of Tar, Water, Nicotine and Carbon Monoxide in Mainstream Tobacco Smoke. Health Canada Test Method T-115.
Heyder, J., 2004. Deposition of inhaled particles in the human respiratory tract and consequences for regional targeting in respiratory drug delivery. Proc. Am. Thorac. Soc. 1 (4), 315–320.
Hirsch, V., et al., 2013. Surface charge of polymer coated SPIONs influences the serum protein adsorption, colloidal stability and subsequent cell interaction in vitro. Nanomedicine 5 (9), 3723–3732.
Ishikawa, S., Nagata, Y., Suzuki, T., 2016. Analysis of Cigarette Smoke Deposition Within an In Vitro Exposure System for Simulating Exposure in the Human Respiratory Tract. Beiträge zur Tabakforschung/Contributions to Tobacco Research 27 (1), 20–29.
Kaur, N., et al., 2010. Evaluation of precision and accuracy of the Borgwaldt RM20S® smoking machine designed for in vitro exposure. Inhal. Toxicol. 22 (14), 1174–1183.
Kesavan, J., Doherty, R.W., 2000. Use of Fluorescein in Aerosol Studies DTIC Document.
Kim, J.S., et al., 2013. Validation of an in vitro exposure system for toxicity assessment of air-delivered nanomaterials. Toxicol. in Vitro 27 (1), 164–173.
Koehler, K.A., et al., 2012. Solid versus liquid particle sampling efficiency of three personal aerosol samplers when facing the wind. Ann. Occup. Hyg. 56 (2), 194–206.
Lízal, F., et al., 2010. Experimental study of aerosol deposition in a realistic lung model. Transactions of the VŠB – Technical University of Ostrava. Mechanical Series 56 (3), 6.

Lizal, F., et al., 2012. Aerosol transport in a model of human lungs. In EPJ Web of Conferences. EDP Sciences.
Majeed, S., et al., 2014. Characterization of the Vitrocell® 24/48 in vitro aerosol exposure system using mainstream cigarette smoke. Chemistry Central Journal 8 (1), 62.
Marple, V.A., Rubow, K.L., Behm, S.M., 1991. A microorifice uniform deposit impactor (MOUDI): description, calibration, and use. Aerosol Sci. Technol. 14 (4), 434–446.
Mertes, P., et al., 2013. A compact and portable deposition chamber to study nanoparticles in air-exposed tissue. Journal of aerosol medicine and pulmonary drug delivery 26 (4), 228–235.
Mullins, B.J., Agranovski, I.E., Braddock, R.D., 2003. Particle bounce during filtration of particles on wet and dry filters. Aerosp. Sci. Technol. 37 (7), 587–600.
Neilson, L., et al., 2015. Development of an in vitro cytotoxicity model for aerosol exposure using 3D reconstructed human airway tissue; application for assessment of e-cigarette aerosol. Toxicol. in Vitro 29 (7), 1952–1962.
Panas, A., et al., 2014. Silica nanoparticles are less toxic to human lung cells when deposited at the air–liquid interface compared to conventional submerged exposure. Beilstein journal of nanotechnology 5 (1), 1590–1602.
Patton, J.S., Byron, P.R., 2007. Inhaling medicines: delivering drugs to the body through the lungs. Nat. Rev. Drug Discov. 6 (1), 67–74.
Paur, H.R., et al., 2008. In vitro exposure systems and bioassays for the assessment of toxicity of nanoparticles to the human lung. Journal Fur Verbraucherschutz Und Lebensmittelsicherheit-Journal of Consumer Protection and Food Safety 3 (3), 319–329.
Paur, H.R., et al., 2011. In-vitro cell exposure studies for the assessment of nanoparticle toxicity in the lung-a dialog between aerosol science and biology. J. Aerosol Sci. 42 (10), 668–692.
Pepper, J.K., Eissenberg, T., 2014. Waterpipes and electronic cigarettes: increasing prevalence and expanding science. Chem. Res. Toxicol. 27 (8), 1336–1343.
Pisinger, C., Døssing, M., 2014. A systematic review of health effects of electronic cigarettes. Prev. Med. 69, 248–260.
Riker, C.A., et al., 2012. *E*-cigarettes: promise or peril? Nurs. Clin. N. Am. 47 (1), 159–171.
Sahu, S., et al., 2013. Particle size distribution of mainstream and exhaled cigarette smoke and predictive deposition in human respiratory tract. Aerosol Air Qual. Res. 13, 324–332.
Scheffler, S., et al., 2015. Cytotoxic evaluation of e-liquid aerosol using different lung-derived cell models. Int. J. Environ. Res. Public Health 12 (10), 12466–12474.
Schripp, T., et al., 2013. Does e-cigarette consumption cause passive vaping? Indoor Air 23 (1), 25–31.
Scian, M.J., et al., 2009. Characterization of a whole smoke in vitro exposure system (Burghart mimic smoker-01). Inhal. Toxicol. 21 (3), 234–243.
Shen, Y., et al., 2016. Transcriptome sequencing reveals e-cigarette vapor and mainstream-smoke from tobacco cigarettes activate different gene expression profiles in human bronchial epithelial cells. Sci. Report. 6.
Thorne, D., Adamson, J., 2013. A review of in vitro cigarette smoke exposure systems. Exp. Toxicol. Pathol. 65 (7), 1183–1193.
Tippe, A., Heinzmann, U., Roth, C., 2002. Deposition of fine and ultrafine aerosol particles during exposure at the air/cell interface. J. Aerosol Sci. 33 (2), 207–218.
Watts, A.B., McConville, J.T., Williams III, R.O., 2008. Current therapies and technological advances in aqueous aerosol drug delivery. Drug Dev. Ind. Pharm. 34 (9), 913–922.
Weidner, C., et al., 2011. Mine Water – Managing the Challenges. parameters affecting na-fluorescein (uranine) detection in mine water tracer tests Aachen, Germany.
Wiegand, H., Meyer, J., Kasper, G., 2015. An electrical conductivity based method of determining the particle deposition rate in air–liquid interface devices. Toxicol. in Vitro 29 (5), 1100–1106.
Yannuzzi, L.A., et al., 1986. Fluorescein angiography complication survey. Ophthalmology 93 (5), 611–617.